Study of the Effect of Graphite Filler on the Vulcanizing Behavior and Properties of Nitrile Rubber and NBR-PVC Blends

[1]D. MURALI MANOHAR*, [2]B.C. CHAKRABORTY AND [3]S. SHAMSHATH BEGUM

[1]Department of Polymer Engineering, B.S.A Crescent Institute of Science & Technology, Chennai, India.

[2]Polymer Nanotechnology Centre, B.S.A Crescent Institute of Science & Technology, Chennai, India.

[3]Department of Polymer Engineering, B.S.A Crescent Institute of Science & Technology, Chennai, India.

ABSTRACT

In search of improved materials for efficient shock and vibration mounts for machineries, graphite loaded NBR and NBR/PVC blend were made and investigated. The scorch time was seen to be reduced and vulcanization rate was enhanced due to graphite inclusion. Scanning electron microscopy images have shown homogenous dispersion of graphite powder. NBR-graphite showed a gradual increase in the hardness, tensile strength, Young's modulus, and tear values with increasing graphite loading. In the case of NBR/PVC-graphite composition, a drop in the tensile strength and increase in the Young' modulus and tear strength was observed. Various mathematical models were used to investigate hardness-Young's modulus relationship and correlation of the modulus with aspect ratio and volume fraction of graphite established. Different equations were also used to predict effect of graphite particle shape factor and hardness of the vulcanised composition on compressive modulus and compared with measured Young's modulus.

Keywords: NBR-PVC blend, Graphite, Vulcanization rate, Hardness, Young's modulus, Compression modulus.

J. Polym. Mater. Vol. **37,** No. 1-2, 2020, 91-107

Correspondence author e-mail: murali@crescent.education
DOI : https://doi.org/10.32381/JPM.2020.37.1-2.7

INTRODUCTION

Nitrile rubber (NBR) and Nitrile-Polyvinyl Chloride (NBR-PVC) blends are well known for some useful properties such as easy mouldability, high strength along with toughness, resistance to hydrocarbon oils, acid, alkali, sea water etc. However, nitrile rubber as such suffers from poor tear strength unless modified suitably [1]. Some examples of chemical modification are hydrogenated nitrile rubber (HNBR) and carboxylated nitrile rubber (XNBR), apart from physical modification, such as blends. NBR-PVC blend is a thermoplastic elastomer with a wide range of flexibility and strength depending on composition. NBR-PVC blends are investigated for vulcanization, physical and mechanical properties by many researchers [2-17]. NBR-PVC blend is compatible in all proportions when acrylonitrile content in NBR is 23 to 45% [2,3]. However, miscibility of a particular blend depends on blending temperature as studied by George *et al.* [4]. Commonly, NBR-PVC blends of 70/30 and 50/50 compositions (by weight) are used commercially.

In order to develop a wide range of shock and vibration mounts, NBR and the NBR-PVC blend systems can be tailored and compounded with various types of fillers. There can be inclusion of spherical shaped carbon black and minerals, layered platelets like graphite, or nanoparticles such as graphene, carbon nanotubes etc [8,11,13,18-20]. Nanocomposites of NBR and NBR/PVC blend with organically modified montmorillonite/cloisite clays are also reported to have high strength and efficient barrier properties [21-23]. Another type of modification reported is formation of Interpenetrating Polymer Network (IPN) of NBR, NBR-PVC blends and NBR-phenolic blend with alkyl methacrylates [24-26].

Reinforcing filler plays an important role in mechanical damping. A plate type filler such as graphite, enhances mechanical damping by converting a compressive deformation to shear deformation of the soft elastomer under a compressive dynamic load as experienced by a machinery mount. In addition, graphite is thermally conducting material. The inclusion of graphite, therefore, could be facilitating higher thermal diffusivity and lower specific heat and hence better heat transfer in the vulcanizing mass [11] and ensures homogeneity in extent of cure in the bulk. The kinetics of vulcanization of elastomers can also be faster due to such conducting inclusions [27-31].

Graphite is characterized by layer type structure with large aspect ratio. It is also known to be a solid lubricant [32], commonly used as a flexible high temperature gasket [33]. Mechanical property and wear resistant of carbon black filled NBR vulcanizate was seen to improve on addition of graphite [34,35]. Mansour *et al.* [11] investigated thermal properties such as thermal conductivity, thermal diffusivity and specific heat for a graphite filled 30/70 NBR/PVC blend while Yang *et al.* [20] studied morphology, rheometry and tensile properties of graphite filled NBR using various forms and shapes of graphite particles. Ismail and Khalaf [29] studied effect of graphite particles on curing, morphology and physico-mechanical properties of SBR. In the study, graphite particles of various sizes from 50 microns to 150 microns and loading up to 150 phr was used. Wang *et al.* [34] studied effect of graphite mainly on tensile and wear

resistance of NBR-Carbon black-graphite system. Agarwal *et al.* [35] studied effect of graphite and graphene on friction and wear rate of NBR.

However, there is no report on quantitative estimation of the effect of graphite particles on vulcanization kinetics, neither any quantitative estimation of dependence of both Young's modulus on hardness of the vulcanizates, aspect ratio and volume fraction of graphite filler and also prediction of compressive modulus of graphite filled NBR and NBR-PVC blends reported in literature so far.

In the present study, NBR and NBR/PVC 50/50 blend vulcanizates filled with varying amount of the graphite powder are prepared and the effect of graphite on NBR and NBR-PVC blend on kinetics of curing process was studied. The effect of graphite inclusion on hardness and mechanical properties of both NBR and NBR-PVC vulcanizates were studied. Relationship of Young's modulus with hardness of the filled vulcanizates, and with volume fraction and aspect ratio of graphite were studied. Two equations were used for prediction of compressive modulus from experimentally determined hardness of the vulcanized compositions and aspect ratio of the graphite particles. The study was carried out to draw a conclusion for the usage of graphite in NBR and NBR-PVC blend vulcanizates for application like machinery mounts.

EXPERIMENTAL

Materials

NBR (KUMHO KNB-35L) and NBR-PVC 50/50 (RUBALOY – 50) blend (termed as NVC in this communication) were obtained from Kumho Petrochemical, Korea and Aarchem Corporation, Chennai, India respectively and used as received. In NBR, acrylonitrile content was 33% and in the NVC blend, the acrylonitrile content in NBR part was 33%. Commercial grade graphite of average particle size of 250 microns was obtained from Loba Chemie, Chennai, India. Other ingredients like sulfur, tetramethyl thiuram disulfide (TMTD), stearic acid and zinc oxide were used as received.

Compounding and Vulcanization

The NBR and NVC blend was masticated in a two-roll mill (Ravi Engineering works, New Delhi, India Model RMMUA-14, friction ratio 1:1.25) until a band was formed in the mill followed by sequential addition of stearic acid, zinc oxide, graphite, TMTD, and sulfur. The mix was homogenized in the mill for 10 minutes at a temperature controlled below 70°C. Finally, the compounded mass was sheeted out as a thin sheet through a 1 mm nip gap of the rolls.

The composition of the NBR and NVC blend with graphite loading is given in Table 1. All ingredients were kept identical for all composition, and only the graphite loading was varied up to 45 phr since, beyond this loading, the integrity of the compound was not proper. The volume fraction of graphite with 10, 20, 30 and 45 phr in NBR-graphite (NBRG) was calculated as 0.042, 0.081, 0.117 and 0.166 respectively. Similarly, the volume fraction of graphite with 10, 20, 30 and 45 phr in NVC-graphite (NVCG) was calculated as 0.047, 0.090, 0.129 and 0.182 respectively. A moving die rheometer (Ektron, Taiwan) was used to study the vulcanization parameters at 150°C such as scorch time (t_s), T_{90}, maximum torque (M_H), and vulcanization time.

Vulcanized sheets were fabricated of size 150 mm x 150 mm having 2 mm thickness and buttons of 30 mm diameter and 12 mm height under a pressure of 15 MPa at 160°C in a hot platen hydraulic press for 8 and 15 minutes respectively. The cured sheets and buttons were further post cured for 8h at 70°C in a hot air oven. The samples were acclimatized at 22°C, 45% RH in the instrumentation enclosure for 24h before any characterization.

TABLE 1. Compounding formulation for NBR and NVC neat and with graphite fillers

Ingredients	Quantity (phr)
NBR / NVC	100
Zinc Oxide	5
Stearic Acid	1
TMTD	1.5
Sulfur	1.5
Graphite	Variable (0, 10, 20, 30, 45)

Characterization Techniques

Mechanical Properties

The tensile and compressive experiments were done using a UTM (Model UTB9251 Dak system Inc., India), according to the procedure given in ASTM D412 and ASTM D575-91(2018) respectively. The Durometer hardness was measured using a hardness tester (BSE SHR-A) in Shore 'A' scale according to ASTM D2240 at five locations in the button and the average of the values was calculated.

Filler dispersion

The dispersion of graphite in the NBR and NVC blend was studied under the scanning electron microscope (CARL ZEISS (USA), (Model: SIGMA WITH GEMINI COLUMN, Resolution 1.5 nm) at an acceleration voltage of 3.0 kV. Tensile fractured samples were used for this analysis.

RESULTS AND DISCUSSION

Vulcanization

The vulcanization of all compounds was carried out at a fixed temperature of 150°C. The vulcanization parameters are listed in Table 2. It can be seen that the time taken for 90% of full torque (T_{90}) is almost same for all graphite loading, except the blank sample. It was observed that the T_{90} is more for NVC blends compared to NBR. This could be due to presence of PVC which restricts the molecular chain movement of NBR by forming C-Cl bond with PVC [7]. The scorch time and cure time observed was similar to that reported in literature [5]. However, the scorch time decreased with the graphite loading as graphite helps in faster attainment of the set temperature. Similar observations were reported in literature for the graphite filled SBR composite [29]. The torque values monotonically increased with increasing graphite content due to increase in stiffness of the compounds. The torque required for the NBR compounds are seen to be much higher than NVC compounds, possibly due to plastic melt flow of PVC at 150°C as PVC may melt at any temperature from 100°C to 216°C depending on polymerization temperature of PVC, processing conditions and additives [36-38]. The vulcanization rate constant for the blank (without Graphite) NBRG00 and NVCG00 were lower than the filled compositions, possibly due to the fact that graphite improves the thermal homogeneity and improved thermal conduction in the mass. However, all graphite containing compositions have almost same or marginally different rate constant. Similar trend was also seen in the values of T_{90} of these compositions as listed in Table 2.

TABLE 2. Vulcanization parameters of Graphite filled NBR and NVC blend

Composition	Scorch Time, T_s	T_{90}, min	Full Torque, dN.m	Cure Rate Index (CRI), min^{-1}	Rate Constant (k), min^{-1} @150°C
NBRG00	2.17	7.86	8.17	17.57	0.0386
NBRG10	2.00	8.00	10.76	16.67	0.0406
NBRG20	1.90	7.92	12.15	16.61	0.0417
NBRG30	1.47	7.57	14.38	16.39	0.0475
NBRG45	1.41	7.42	15.76	16.64	0.0498
NVCG00	2.70	9.22	4.91	15.34	0.0352
NVCG10	2.06	8.31	7.26	16.00	0.0431
NVCG20	2.00	8.48	8.40	15.43	0.0417
NVCG30	1.87	8.37	9.49	15.38	0.0458
NVCG45	1.80	8.42	10.87	15.11	0.0486

The curing rate index (CRI) is an indirect parameter to assess the vulcanization rate and is given by:

$$CRI = \frac{100}{(T_{90} - T_S)} \quad (1)$$

The CRI values listed in Table 2 show that the index is almost same for all graphite loaded compositions with both NBR and NVC blend. Kinetics of vulcanization was determined taking the T_{25} to T_{50} portion of the vulcanization curves. The rheographs of NBR and NVC blend without and with graphite is shown in Figure 1 and Figure 2 respectively. The four representative kinetic plots according to Eq. 2 are shown in Figure 3 and Figure 4. The first order rate constant was determined from the following simple rate equation [7]:

$$\ln (M_\infty - M_0) = -k (t - t_s) + (M_\infty - M_0) \quad (2)$$

where, M_∞ = Maximum Torque, M_0 = Minimum Torque, M = Torque at time t, k is the first order rate constant and t_S is the scorch time.

The vulcanization process is quite similar to most commonly used vulcanization of rubbers, as indicated by cure time and CRI values. The reaction rate of neat NBR (NBRG00) and the neat blend NVC (NVCG00) were almost of the same order as the literature value of self-crosslinking in case of blending of NBR with PVC and also conventional sulfur vulcanization [5-7].

Figure 3 and Figure 4 shows plot of $\ln(M_\infty - M_0)$ vs $(t\text{-}t_s)$ for NBR and NVC compositions. The expression in Eq.1 arises from the assumption that the increase in torque is proportional to the fractional conversion, a of curing reaction, as shown below:

$$\alpha = \frac{M - M_0}{M_\infty - M_0}$$

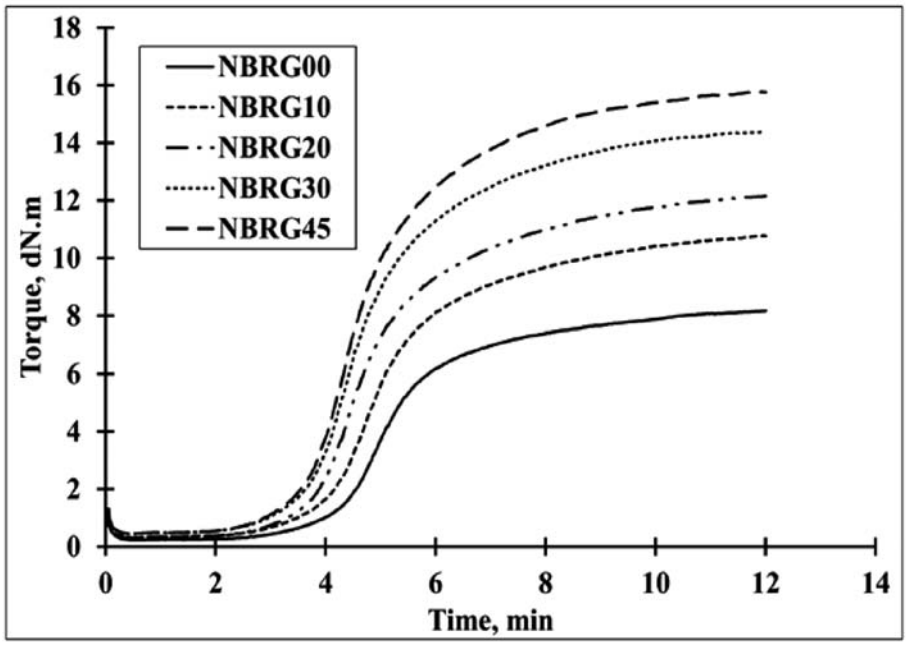

Fig. 1. Rheographs of sulfur vulcanization of NBR and Graphite filled compounds.

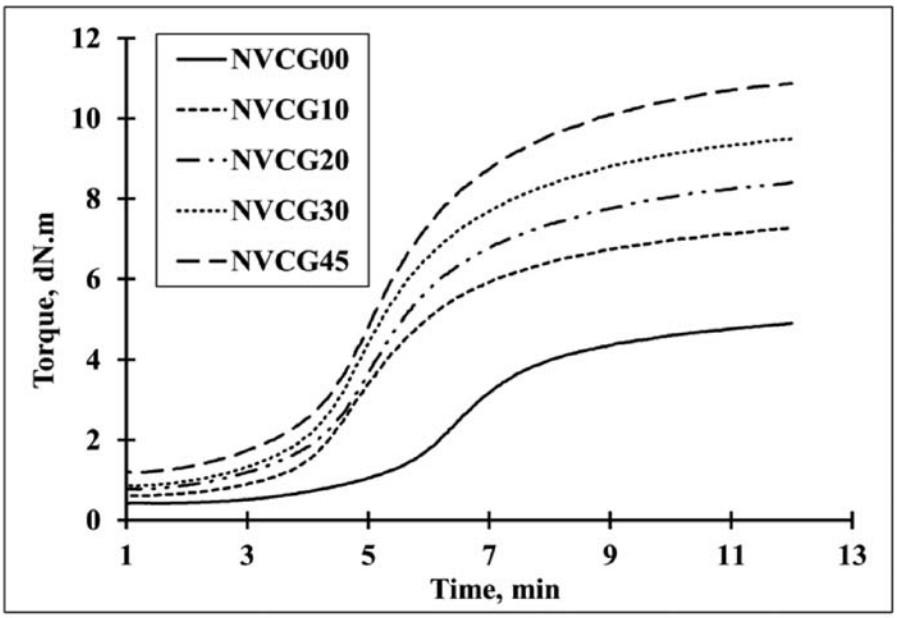

Fig. 2. Rheographs of sulfur vulcanization of NVC blend and graphite filled Compounds.

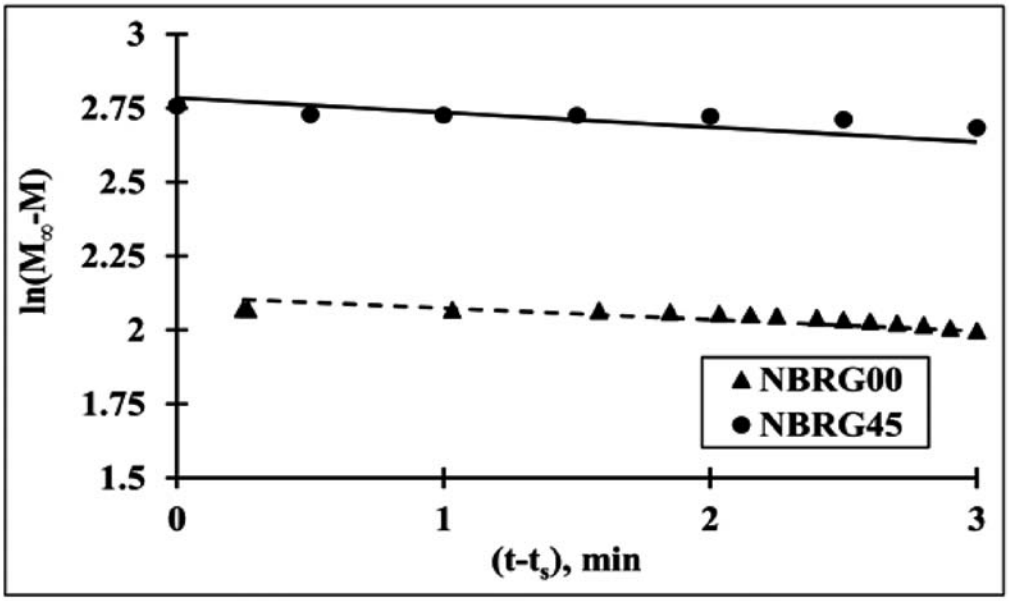

Fig. 3. First order reaction kinetics plot for NBRG00 and NBRG45.

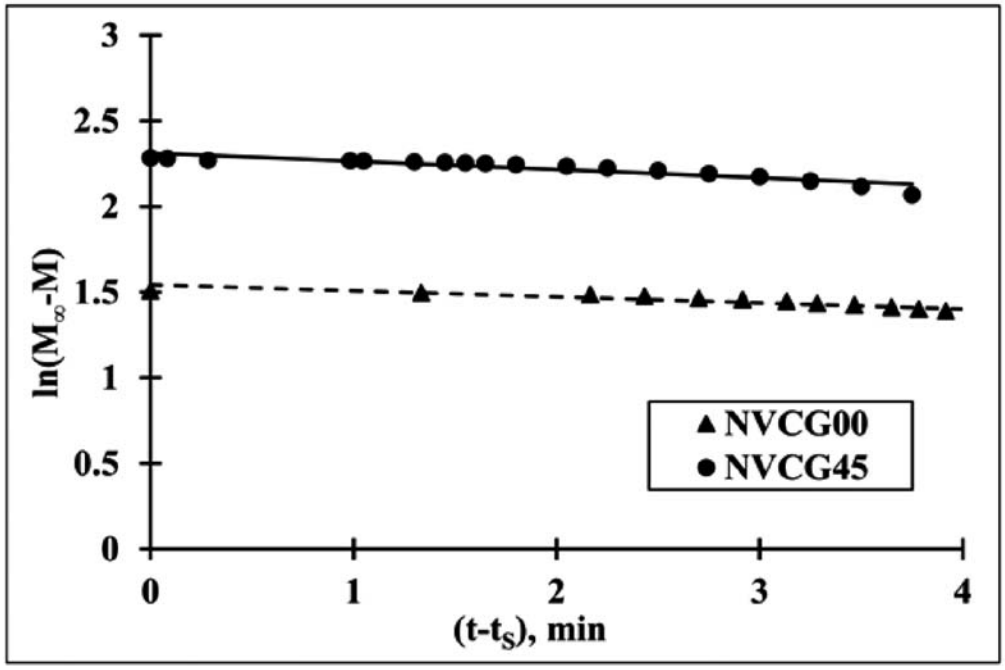

Fig. 4. First order reaction kinetics plot for NVCG00 and NVCG45.

The time axis is ($t-t_s$) to eliminate the scorch period for rate calculation. The slope of each graph represents first order rate constant (k) and the intercept is $\ln(M_\infty-M_0)$. The minimum torque (M_0) is taken at the scorch time (t_s). The first order plot in Figure 3 for NBR compositions has a better fit of experimental data compared to NVC compositions in Figure 4. The minute non-linear behaviour in Figure 4 could be attributed to the additional self-cross-linking of NBR with PVC as studied by Manoj *et al.* [7]. It can be seen that the slope of neat NVC (NVCG00) in Figure 4 is somewhat less than that of neat NBR (NBRG00) in Figure 3, which means that the rate constant is higher for NBR compared to the NVC blend. This may be due to the presence of PVC in NVC blend, which affects the overall rate constant because of a slower self-cross-linking step [7]. In addition, graphite containing compositions NBRG45 has slightly higher slope than neat NBRG00 as in Figure 3 indicating higher rate of vulcanization on addition of graphite. Similar trend is also seen on comparison of NVCG00 and NVCG45 in Figure 4.

Morphology

Morphology of the compositions with graphite were studied by SEM. Figure 5 (A), (B), (C) and (D) represent SEM micrographs of 10 phr and 20 phr graphite containing NBR and NVC blend vulcanizates respectively. The lateral dimension of the platelets was on an average 5.5 microns as calculated from NVC blend. The distribution of the graphite plates was quite homogeneous with very close crowding even for 20 phr content in both NBR and NVC blend. The random orientation of the graphite particles is seen in the figure in the plane of the rubber sheet. Some agglomeration is also visible in the higher loading as in Figure 5 (D). The average aspect ratio of the graphite platelets is about 7.00 computed approximately using SEM micrograph as shown in Figure 5 (C) & (D).

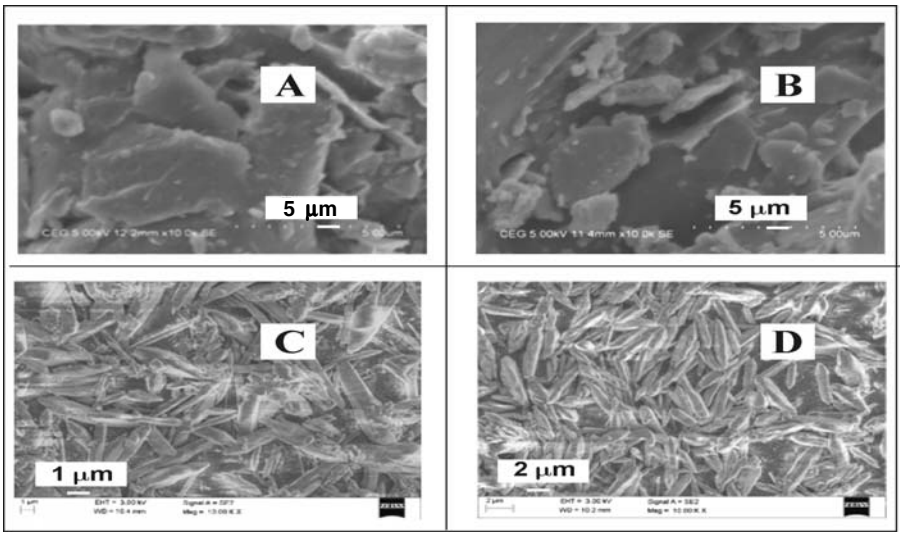

Fig. 5. Morphology of graphite filled NBR and NVC Composition, (A) NBRG20, (B) NBRG45 (C) NVCG10 and (D) NVCG20.

Hardness, Tear and Tensile Properties

Durometer hardness of NBR and NVC compositions increased from gum vulcanizate to 45 phr graphite filled composition, in a linear relationship with graphite loading, as seen in Figure 6. The scatter of data is very less in each volume fraction, due to a uniform particle distribution. The rate of increase in hardness for NBR is more than in case of NVC compositions. This can be attributed to the plasticization of PVC by the graphite and this results in higher lateral conversion of the indentation force and hence low indentation hardness.

Table 3 lists the tear and tensile properties of the NBR and NVC based compositions. The Young's modulus here is defined as the tensile modulus at 1% strain, and the modulus is independent of strain up to about 4-5% for all the compositions. The incorporation of graphite has resulted in a more reduction of 100% modulus compared to corresponding 1% modulus for both NBR and NVC compositions. It is also seen that the reduction is not that sharp for NBR-graphite compositions, as in NVC-graphite. While the ratio of 100% Modulus to 1% Modulus for NBR-graphite is changed from 0.4 to 0.3 for increase in graphite content from 10 phr to 45 phr, the same ratio for NVC-graphite changes from 0.6 to 0.35. This also could be due to plasticizing of PVC part by the graphite particle.

TABLE 3. Tear strength and Tensile properties of NBR and NVC blend with graphite filler

Designation	UTS MPa	% Elongation at break	Young's Modulus @ 1% strain, MPa	Young's Modulus @100% strain, MPa	Tear Strength kN/m
NBRG00	1.76	214.00	2.51	1.18	8.76
NBRG10	2.40	271.40	3.63	1.40	14.16
NBRG20	2.30	236.60	4.41	1.56	17.28
NBRG30	2.61	194.30	6.08	2.03	30.65
NBRG45	3.03	183.80	8.27	2.49	47.71
NVCG00	15.22	388.00	4.81	3.09	31.43
NVCG10	14.41	381.89	7.52	4.21	50.25
NVCG20	11.01	276.44	10.01	4.88	52.92
NVCG30	11.69	285.36	12.51	5.80	51.40
NVCG45	12.67	263.22	20.97	7.32	53.47

The Young's modulus is progressively increasing with the graphite content. The modulus is directly related to hardness of an elastomer as studied by many researchers [39-44]. Tensile strength of NBR based composites are consistently increasing with graphite loading, although the improvement in strength is not much, in fact not even twice the gum

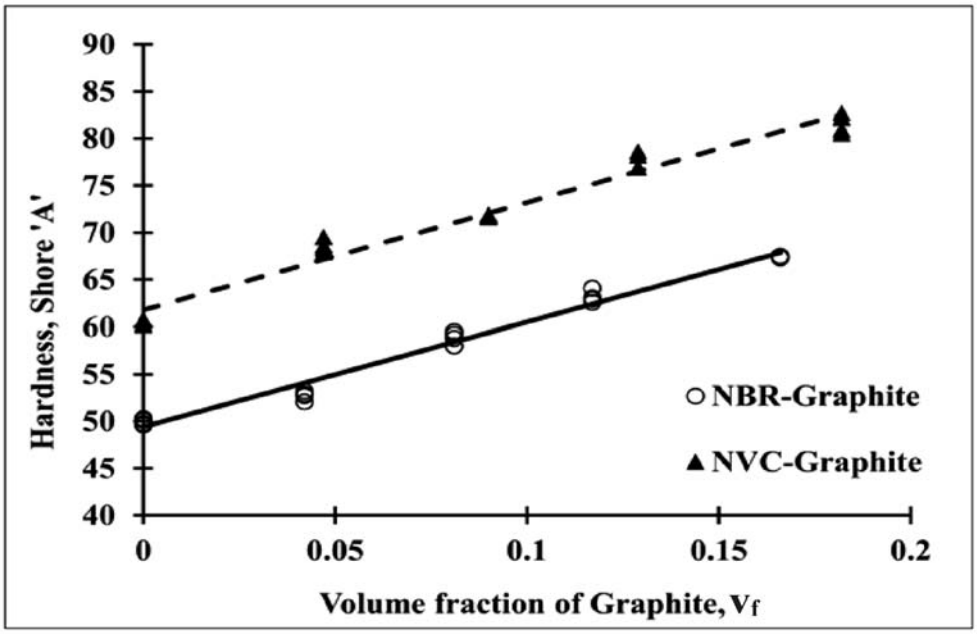

Fig. 6. Dependence of hardness on graphite loading in NBR and NVC blend vulcanizates.

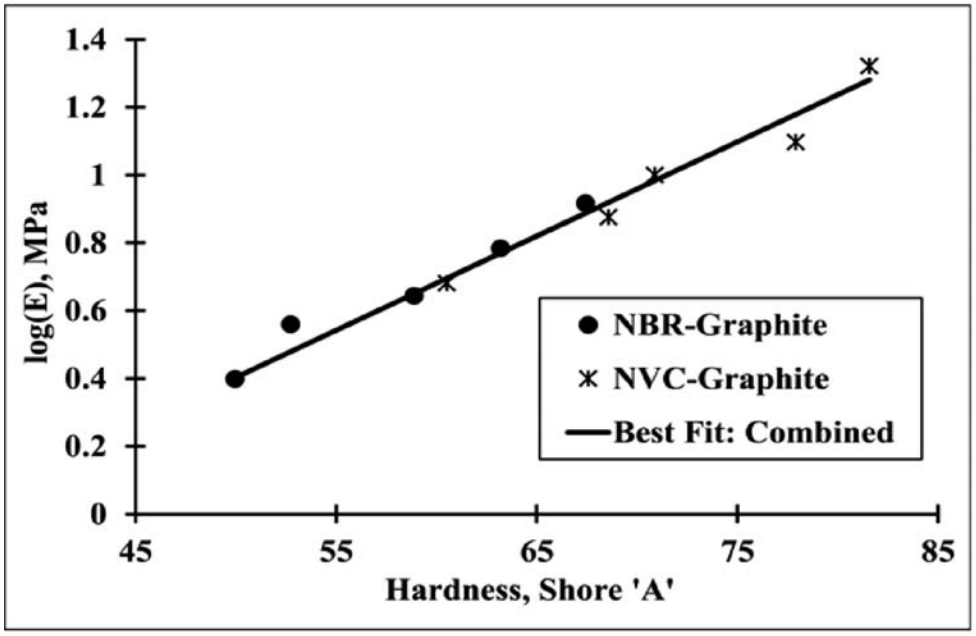

Fig. 7. Hardness – Young's Modulus relationship of graphite filled NBR and NVC blend.

vulcanizate. Therefore, graphite has limited reinforcing effect to the rubber. However, the tensile strength of NVC blend vulcanizate decreased with graphite loading. It is observed that the strength of all graphite loaded NVC composites are almost same and much lower

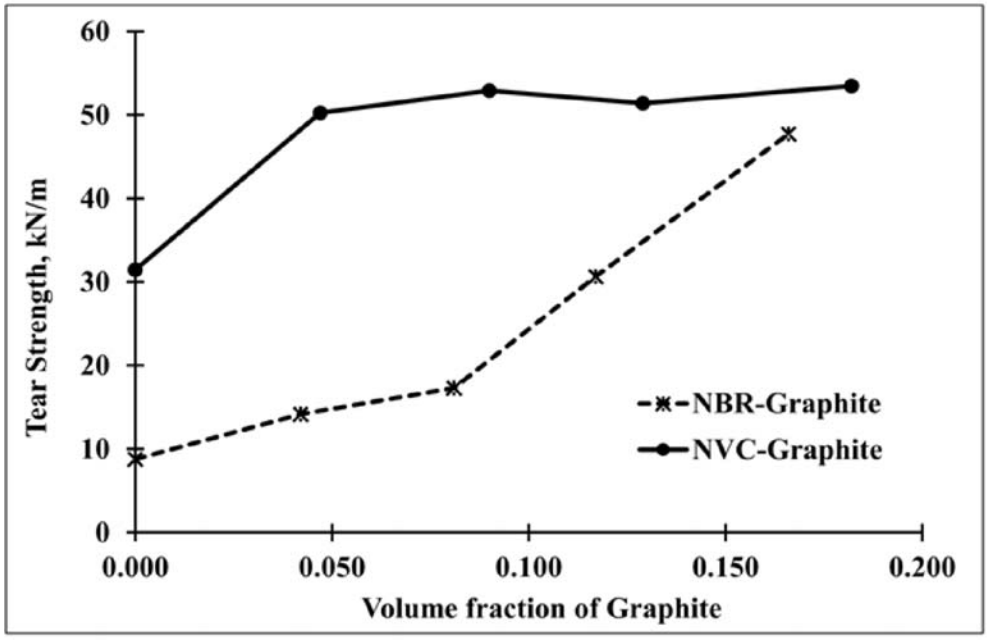

Fig. 8. Variation of tear strength of NBR and NVC vulcanizate on graphite inclusion.

than the gum vulcanizate. This indicates the uniform distribution of graphite which act as an additional plasticizer to the PVC part of the NVC matrix. The same trend has been observed in another study [39].

For present formulations, the hardness is directly proportional to log of Young's modulus as seen in Figure 7. The relation is similar to that suggested by Qi *et al.* [40].

The present empirical relation is given as:

$$Log(E) = 0.0278S - 0.98 \quad (3)$$

The above relation is applicable to both NBR and NVC blend vulcanizates with graphite inclusion. It should be noted that the relationship is valid within the limits of hardness values 50 to 85 Shore 'A'.

The tear strength of the NBR vulcanizate is generally much lower than that of NVC composition as seen in Table 3. A comparison of the tear strengths is graphically shown in Figure 8. However, tear strength of NBR is significantly enhanced to twice the value on addition of 20 phr graphite (NBRG20) and almost 5 times on addition of 45 phr graphite (NBRG45). This enhancement is in line with the change in ultimate tensile strength, whereas, the tear strength of NVC vulcanizate has increased for NVCG10 but did not enhanced on further increase in graphite

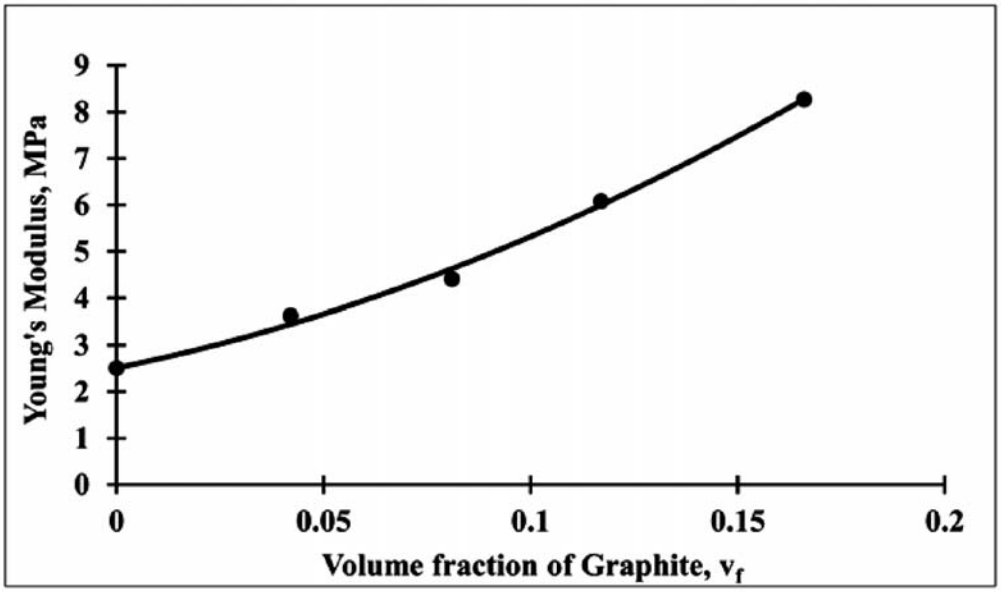

Fig. 9. Variation of Young's Modulus of NBR vulcanizates on graphite reinforcement taking aspect ratio of graphite as 7.00.

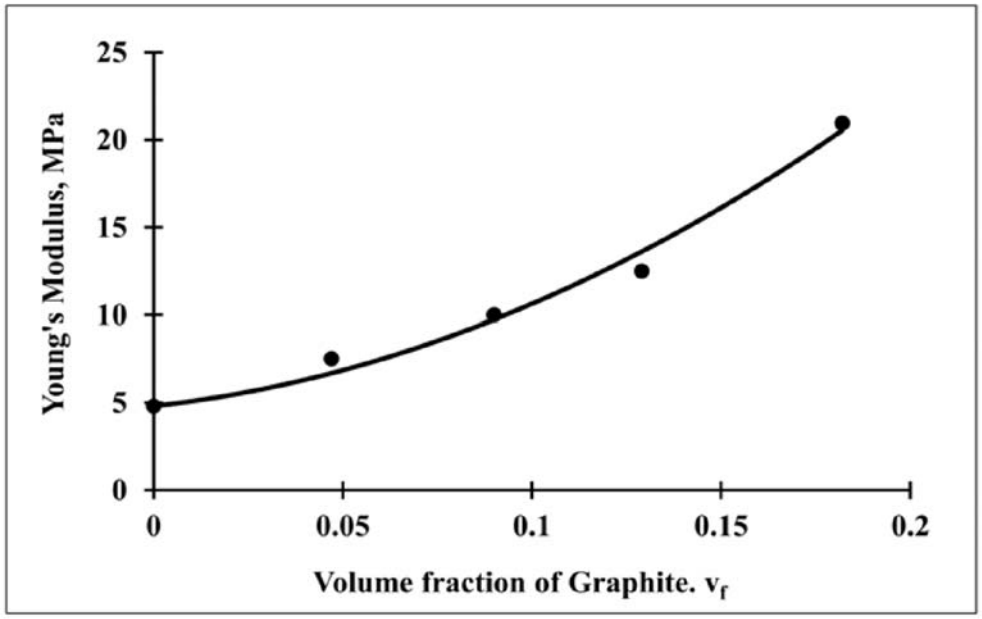

Fig. 10. Variation of Young's Modulus of NVC vulcanizates on graphite reinforcement taking aspect ratio of graphite as 7.00.

loading. This is almost same as the trend observed for tensile strength. In general, it is observed that the presence of PVC in NVC blend has resulted in drastic improvement in tear strength compared to NBR.

Whereas change in Young's Modulus is more for NVC blends on graphite inclusion. Quantitatively, the change is about 4 times in NVC compared to about 3 times in NBR. Since Young's modulus is calculated at a very low strain in tension (1% in present case), the effect of plasticization action of graphite for PVC is not expected. This results in progressively higher Young's modulus on increasing graphite content for NVC, unlike ultimate tensile strength or tear strength, where, the strains in tension are significantly high. Figure 9 and Figure 10 show the effect of filler volume fraction on Young's modulus of NBR and NVC vulcanizates respectively. It is seen that the relations have very good fit for a second order polynomial and the general relationship of the Young's modulus and volume fraction of a filler having an aspect ratio >>1 (rod shaped particle) is given by Guth[41] as:

$$\frac{E}{E_0} = 1 + a_1\phi^2 v_f^2 + a_2\phi v_f \qquad (4)$$

where, E_0 is the Young's modulus in MPa, of the neat vulcanizate without filler, ϕ and v_f are the shape factor (length/breadth) and volume fraction of the filler particle respectively and a_1, a_2 are constants depending on the rubber-filler interaction. Guth [41] suggested the values of a_1 = 1.62 and a_2 = 0.67, for rod like inclusion uniformly distributed in the matrix. The coefficients suggest that the increase in modulus is more rapid than linear variation. For ϕ = 1, we obtain the case for spherical inclusion, such as carbon black particles, as observed by Guth[41].

In the present systems, the shape factor of graphite particles is taken as 7.00 as stated earlier. Consequently, the empirical relationships for NBR and NVC vulcanizates with graphite loading are given as:

For NBR-graphite system:

$$\frac{E}{E_0} = 1 + 0.854\phi^2 v_f^2 + 0.97\phi v_f \qquad (5)$$

For NVC-graphite system:

$$\frac{E}{E_0} = +1 + 1.459\phi^2 v_f^2 + 0.706\phi v_f \qquad (6)$$

For above empirical relationships as Eqs. 5 and 6, a_1 and a_2 values were taken as 1.62 and 0.67 respectively for rod like inclusion as suggested by Guth since the graphite particles are rod shaped as seen in SEM image (Figure 5). The aspect ratio ϕ of the graphite filler was calculated from the image in Figure 5 as average 7.0 and the volume fraction v_f of graphite in each composition is as mentioned in experimental section above. It is seen from Table 3 that the increase in modulus of NVC-graphite compositions are marginally higher than the corresponding increase in modulus for NBR-graphite compositions and this is reflected in the values of the polynomial coefficients in Eqs. 5 and 6.

Compressive Modulus predicted vs experiment value

Ideally, tensile and compression modulus should be same and is termed as Young's Modulus. However, in a thicker sample used for compression experiment, a uniform compression will lead to mode conversion from

compressive strain to shear strain as the load-free surface is large and Poisson's ratio of rubbers being nearly 0.5. As per ASTM standard, a compression experiment is done on a button of 28 mm diameter and 12 mm thickness, having very small aspect ratio (D/4h) of 0.583 and hence the shear deformation is significant. Consequently, the compressive modulus is lower than Young's modulus at a strain level sufficient to cause lateral deformation. Rocard [45] and Kunz & Studer [46] separately studied the relation of hardness and compressive modulus of common rubbers using samples of low shape factor (0.55). their relationships are described below:

Rocard [45] :

$$E_c = \frac{H^{1.9}}{972.021}\left[\frac{1+k_1 S^2}{+k_2 S^2} + 2S^2\right] MPa \qquad (7)$$

where H is hardness in Shore 'A', S = aspect ratio (D/4h), k_1 = 4.8 and k_2 = 4 for low shape factor.

Kunz & Studer[46] :

$$E_c = \left[\frac{1-\nu^2}{2RC_3}\right]\frac{C_1 + C_2 S_A}{100 - S_A} \quad N/m^2 \qquad (8)$$

where, C_1 = 0.549 N, C_2= 0.07516 N and C_3 = 0.025 mm, while ν is the Poisson's Ratio, E_c is the elastic modulus in compression and R is the radius of the indenter. In the present case, R= 0.395 mm as in durometer Shore 'A' indenter and Poisson's ratio (ν) of rubber is taken as 0.5.

The predictive compressive modulus (E_c) of NBR and NVC vulcanizates with and without graphite inclusion were calculated using both Eqs.7 and 8 and these are compared to the measured Young's modulus (E) of the corresponding compositions. The results are presented in Figure 11 and Figure 12 as the ratio E_c/E as a function of volume fraction of Graphite. It can be seen that the ratio continuously decreases with increase in graphite content and at about 17-18% (by Volume) inclusion, predicted

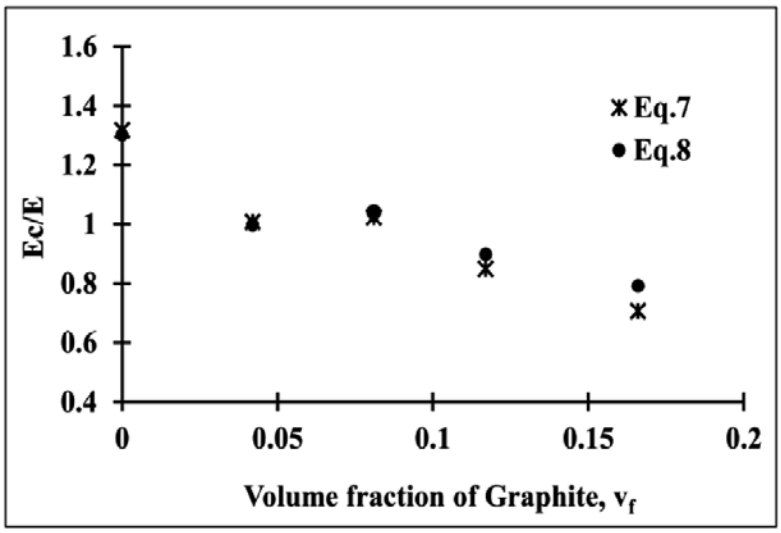

Fig. 11. Ratio of compressive modulus Ec to Young's modulus E (@1% strain) for NBR-graphite.

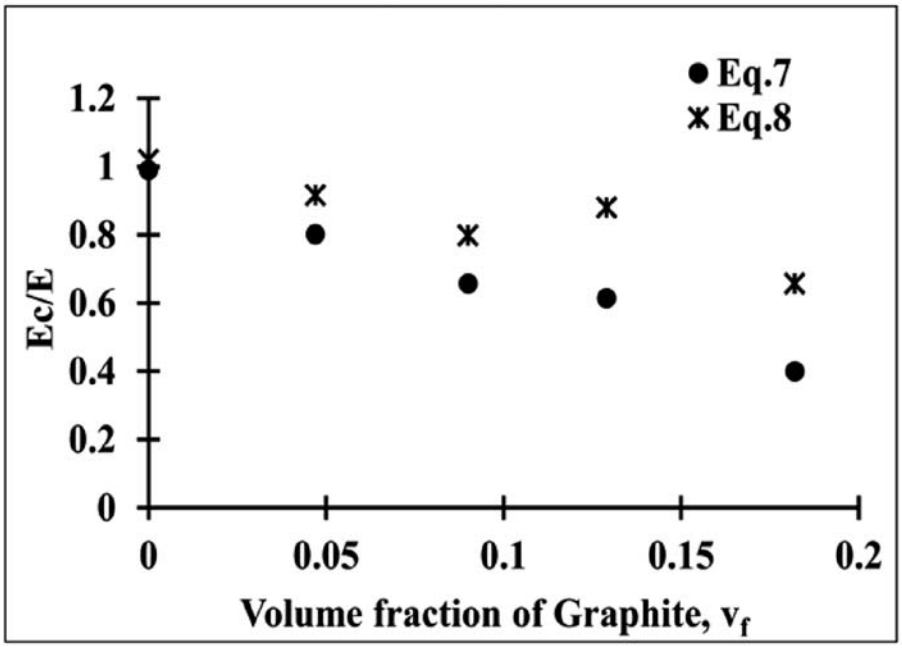

Fig. 12. Ratio of compressive modulus E_c to Young's Modulus E (@1% strain) for NVC-graphite.

compressive modulus is about 75-80% of the Young's modulus (considering Eq.8) for NBR-graphite and about 50% for NVC-graphite.

The ratio of compressive modulus to Young's modulus (Ec/E) for graphite filled NVC compositions are predicted to be less compared to those for graphite filled NBR. This could be due to larger lateral deformation of the sample under compression due to lubrication of PVC by graphite. Since the compressive modulus is calculated using hardness data, it is seen in Figure 6 that the hardness improves more in case of NBR compared to NVC with the variation in the graphite volume fraction.

CONCLUSION

Graphite filled NBR and NBR-PVC 50/50 (NVC) blend were investigated in quest of a suitable material for machinery mount application. Graphite inclusion in NBR and in NBR-PVC blend resulted change in kinetics of vulcanization and mechanical properties. There is a significant improvement in tear strength, hardness and Young's modulus for both NBR and the NVC blends on graphite inclusion. However, tensile strength of NVC blend is decreased on graphite addition. Young's modulus of vulcanized NBR and NVC blend filled with graphite is seen to be non-linearly varying with volume fraction and aspect ratio of graphite.

Prediction of compressive modulus of the compositions was done using two different equations from literature [45,46]. NVC-graphite showed overall lower compressive modulus (predicted) compared to the measured Young's Modulus, possibly due to considerable shear

deformation as a result of plasticizing effect of graphite on PVC in the NVC composition during compression.

REFERENCES

1. H.L. Varghese, S.S. Bhagawan, N. Prabhakaran and S. Thomas, *Mater. Lett.* (1995) 24, 333-339.
2. G. A. Zakrzewski, *Polymer* (1973) 14, 348.
3. L. M. Robeson, *Polym Engg Sci.* (1984) 24(8), 587-597.
4. K.E. Geprge, R. Joseph and D.J. Francis, *J. Appl. Polym. Sci.* (1986) 32, 2867-2873.
5. A.A. Shokri1, G. Bakhshandeh and T.D. Farahani, *Iran. Polym. J.* (2006) 15 (3), 227-237.
6. M.H. Al-Maamori, A.I. Al-Mosawi, S.A. Abdulsada and H.A. Yasser, *EC Chemistry* (2015) 1.1, 25-29.
7. N.R. Manoj and P. P. De, *Polymer* (1998) 39(3), 733 -741.
8. V.L.C. Lapa, L.Y. Viscont, J.E.S. Affonso and R.C. R. Nunes, *Polym. Test.* (2002) 21, 443-447.
9. M. Hafezi, S.N. Khorasani and F. Ziaei, *J. Appl. Polym. Sci.* (2006) 102, 5358-5362.
10. M. Hafezi, S.N. Khorasani, F. Ziaei and H.R. Azim, *J. Elastom. Plast.* (2007) 39, 151-163.
11. S.A. Mansour, M.E. El-Ghoury, E. Shalaan, M.H.I. El Eraki and E.M. Abdel-Barry, *J. Appl. Polym. Sci.* (2010) 116, 3171-3177.
12. N.L. Thomas and R.J. Harvey, *Progress in Rubber and Plastics Technology* (2001) 17(1), 1-12.
13. S.D. Kaushik, *J. Applicable Chem.* (2017) 6(4), 628-631.
14. F.A. Passador and L.A. Pessan, *Polymeros: Ciência e Technologia* (2006) 16(3), 174-181.
15. E.S. Fathy, M.Y. Elnaggar and M.M. Hassan, *J. Rad. Sci. Applic.* (2018) 31(1), 1 - 11.
16. X.Y. Shi, B. Weina and Z. Shugao, *J. Appl. Polym. Sci.* (2011) 120, 1121-1125.
17. M.H. Al-Maamori, A.I. Al-Mosawi and H.A. Yasser, *American Journal of Materials Research,* (2015) 2(3), 31-34.
18. A. Hajibaba, G. Naderi, M. Ghoreishy, G. Bakhshandeh and M.R. Nouri, *Iran Polym J.* (2012) 21, 505-511.
19. A. Hajibaba, G. Naderi, E. Esmizadeh and M.H.R. Ghoreishy, *J. Compos. Mater.* (2012) 48(2), 131-141.
20. Jian Yang, Ming Tian, Qing-Xiu Jia, Li-Qun Zhang, Xiao-Lin Li, *J Appl Polym Sci.* (2006) 102, 4007-4015.
21. L. Hanhua, W. Li and S. Guojun, *Iran Polym J.* (2010) 19(1), 39-46.
22. K.K. Sadasivunia, D. Ponnamma, S. Thomas and Y. Grohens, *Prog. Polym. Sci.* (2014) 39, 749-780.
23. L. Bokobza, *Journal of Carbon Research,* (2017) 3(2), 10.
24. A. Mathew, B. C. Chakraborty and P. C. Deb, *J. Appl. Polym. Sci.* (1994) 53, 1107-1114.
25. M. Patri, A. B. Samui, B. C. Chakraborty and P. C. Deb, *J. Appl. Polym. Sci.* (1997) 65, 549-554.
26. A.B. Samui, U.G. Suryavanshi, M. Patri, B.C. Chakraborty and P.C. Deb, *J. Appl. Polym. Sci.* (1998) 68, 255-262.
27. S.H. Chouch and D.H. Chang, *J. Appl. Polym. Sci. (1996) 61, 449-454.*
28. R. Ding and A. 1. Leonov, *J. Appl. Polym. Sci.* (1996) 61,455-463.
29. M. N. Ismail and A. I. Khalaf, *J. Appl. Polym. Sci.* (2011) 120, 298-304.
30. M. Sadeghalvaad, E. Dabiri, S. Zahmatkesh and P. Afsharimoghadam, *J. Nanostruct (*2019) 9(3), 453-467.
31. B. Mensah, K.C. Gupta, G. Kang, H. Lee and C. Nah, *Polym. Test.* (2019) 76, 127-137.
32. D.D.L. Chung, *J Mater Sci (2002) 37 1475-1489.*
33. Noshirwaan Aibada, M. Ramachandran, Krishna Kumar Gupta, P. P. Raichurkar, *International Journal on Textile Engineering and Processes* (2017) 3, Issue 1.

34. Lei Lei Wang, Li Qun Zhang, Ming Tian, *Materials and Design* (2012) 39 450-457.

35. N. Agrawal, A.S. Parihar, J.P. Singh, T.H. Goswami and D.N. Tripathi, *International Conference on Nanomaterials and Technologies (CNT 2014), Elsevier,* (2015) 2211-8128.

36. https://en.wikipedia.org/wiki/Polyvinyl_chloride

37. F.P. Reding, E.R. Walter and F.J. Welch, *J. Polym. Sci.* (1962) 56(163), 225-231.

38. L.C. Uitenham and P.H. Geil, *J Macromol Sci B, (1981) 20(4), 593-622.*

39. I.M. Meththananda, Sandra Parker, Mangala P. Patel, Michael Braden*, Dental Materials* (2009) 25, 956-959.

40. H.J. Qi, K. Joyce and M.C. Boyce, *Rubber Chem. Technol.* (2002) 76, 419-435.

41. E. Guth, *J. Appl. Phys.* (1945) 16, 20-25.

42. A.N. Gent, *Trans. Inst. Rub. Ind.* (1958) 34, 46-57.

43. B.J. Briscoe and K. Savio Sebastian, *Rubber. Chem. Technol. (1993)* 66, 827-836.

44. BS 903 Methods of testing vulcanised rubber Part 19 (1950) and Part A7 (1957).

45. Y. Rocard, *J. Phys. Radium* (1937) 8(5), 197-203.

46. J. Kunz and M. Studer, *Kunststoffe International* (2006) 6, 92-94.

Received: 20-12-2019

Accepted: 28-01-2020